MUCOSAL IMMUNOLOGY

Dietary antigens limit mucosal immunity by inducing regulatory T cells in the small intestine

Kwang Soon Kim,[1,2] Sung-Wook Hong,[1,2] Daehee Han,[1,2] Jaeu Yi,[1,2] Jisun Jung,[1,2] Bo-Gie Yang,[1,2] Jun Young Lee,[1,2] Minji Lee,[1,2] Charles D. Surh[1,2,3]*

Dietary antigens are normally rendered nonimmunogenic through a poorly understood "oral tolerance" mechanism that involves immunosuppressive regulatory T (T_{reg}) cells, especially T_{reg} cells induced from conventional T cells in the periphery (pT_{reg} cells). Although orally introducing nominal protein antigens is known to induce such pT_{reg} cells, whether a typical diet induces a population of pT_{reg} cells under normal conditions thus far has been unknown. By using germ-free mice raised and bred on an elemental diet devoid of dietary antigens, we demonstrated that under normal conditions, the vast majority of the small intestinal pT_{reg} cells are induced by dietary antigens from solid foods. Moreover, these pT_{reg} cells have a limited life span, are distinguishable from microbiota-induced pT_{reg} cells, and repress underlying strong immunity to ingested protein antigens.

The ingestion of certain foods can trigger an immune reaction, ranging from mild allergy to anaphylaxis, in a fraction of the population. How dietary antigens (Ags) are normally rendered nonimmunogenic through oral tolerance is poorly understood, but it is known to require the participation of regulatory T (T_{reg}) cells expressing the transcription factor Foxp3 (*1*, *2*). Two types of Foxp3$^+$ CD4$^+$ T_{reg} cells exist: the thymic T_{reg} (tT_{reg}) cells that develop from hematopoietic progenitors in the thymus, and the peripheral T_{reg} (pT_{reg}) cells that develop extrathymically from conventional T cells (*3*–*6*).

pT_{reg} cells are abundant in the intestine but not in the secondary lymphoid tissues (*7*), implying that pT_{reg} cells develop in response to enteric Ags derived from the commensal microbiota and/or food. In the colon, the intestinal microbes induce the development of pT_{reg} cells, and these cells are depleted in germ-free (GF) mice (*7*–*9*). However, GF mice possess normal numbers of pT_{reg} cells in the small intestine (*7*), the origin of which has yet to be documented. Oral administration of a nominal protein Ag under experimental conditions can induce a fraction of Ag-specific CD4$^+$ T cells to differentiate into pT_{reg} cells (*10*), but whether pT_{reg} cells are generated in response to a typical diet thus far has been unknown. To address this, we studied the effect of depleting dietary Ags by raising mice on a chemically defined elemental diet devoid of macromolecules. We derived such Ag-free (AF) mice by producing offspring from GF mice that were weaned onto and subsequently raised on the elemental Ag-free diet (table S1) (*11*).

Young adult AF C57BL/6 (B6) mice appeared healthy, were similar in size and weight, and possessed comparable serum biochemical and metabolic markers, except for moderately low levels of vitamin A and D, albeit within the acceptable ±100% range relative to those of specific pathogen-free (SPF) and GF B6 mice (fig. S1). As previously reported (*12*, *13*), AF mice had lower serum immunoglobulins, normal-sized spleens, and lower lymphocyte counts in the small intestinal lamina propria (siLP), but not in the colonic lamina propria (cLP), relative to SPF mice (fig. S2). The hypocellularity in the siLP was particularly pronounced for CD4$^+$ T cells because of the depletion of memory-phenotype (CD44^{hi} CD62L^{lo}) cells, including Tbet$^+$ cells (Fig. 1, A and B, and fig. S4); CD4$^+$ T cell counts in the cLP were normal, but memory-phenotype CD4$^+$ T cells were significantly decreased, as in GF mice (figs. S3 and S4). These phenotypes suggest that local activation of CD4$^+$ T cells in the small intestine is driven mainly by dietary Ags, whereas in the colon it is induced by the microbiota.

Foxp3$^+$ CD4$^+$ T_{reg} cell counts in adult AF B6 mice were also normal in the periphery but much reduced in the intestine compared with those of SPF mice. In the cLP, AF mice resembled GF mice and possessed about half the percentages and total numbers of T_{reg} cells relative to SPF mice (Fig. 1C and fig. S5B). In the siLP of AF mice, despite higher percentages, total numbers of T_{reg} cells were about one-fifth those of GF and SPF mice (Fig. 1, C and D). To distinguish between tT_{reg} and pT_{reg} cell subsets, the expression of neuropilin-1 (Nrp-1) was analyzed. As reported previously (*7*), pT_{reg} cells expressing little Nrp-1 (Nrp-1^{lo}) were largely absent in the spleen and lymph nodes but made up 50 to 70% of T_{reg} cells in the siLP and cLP in SPF mice; in GF mice, pT_{reg} cells were rare in the cLP but prominent in the siLP (Fig. 1E). In contrast, in AF mice, Nrp-1^{lo} pT_{reg} cells were depleted in both the siLP and cLP (Fig. 1E). Intestinal Nrp-1^{lo} pT_{reg} cells in SPF mice, but not the few remaining in AF mice, also expressed higher levels of CTLA-4 and the cytokine interleukin (IL)–10 than Nrp-1^{hi} tT_{reg} cells did (figs. S6 and S7). IL-10$^+$ Foxp3$^-$ CD4$^+$ cells, which were presumably type 1 regulatory T (T_r1) cells, were present in low numbers in the gut of SPF but not of GF and AF mice, and T_r1 cells expressed lower levels of IL-10 than did Foxp3$^+$ T_{reg} cells (fig. S7, A and B). Together, these results indicate that dietary Ags induce the development of most of pT_{reg} cells in the siLP under normal conditions, and pT_{reg} cells appear more essential than T_r1 or tT_{reg} cells in regulating immune responses to dietary Ags.

To assess the relative contributions of milk versus solid-food Ags in inducing the development of intestinal pT_{reg} cells, neonatal and adult mice were examined. pT_{reg} cells in the siLP were sparse before weaning in AF, GF, and SPF B6 mice but became prominent shortly after weaning these mice onto a normal chow diet (Fig. 2A and fig. S8). Furthermore, the deprivation of dietary Ags, accomplished by weaning neonatal GF mice onto the Ag-free diet or onto an "amino acid" diet that was devoid of proteins, prevented efficient development of pT_{reg} cells in the siLP (Fig. 2, B and C); in addition, unlike regular AF mice, these mice had normal levels of serum vitamin A, which promotes the generation of pT_{reg} cells through its metabolite retinoic acid (fig. S9, A and B) (*14*, *15*). Moreover, the administration of retinoic acid to adult AF mice did not result in the emergence of siLP pT_{reg} cells (fig. S9C). Hence, the majority of pT_{reg} cells in the siLP develop in response to Ags derived from proteins in a solid-food diet. As expected, siLP pT_{reg} cells underwent rapid turnover and had a short life span when deprived of food Ags. Thus, when adult (8-week-old) GF mice were placed on the Ag-free diet, the fraction of siLP pT_{reg} cells decreased considerably (by ~40%) after ~4 weeks (Fig. 2D). These results indicate that pT_{reg} cells in the siLP are continuously generated and replaced in response to dietary Ags, with a half-life of 4 to 6 weeks.

In addition to dietary Ags, commensal microbial Ags presumably contribute to the generation of pT_{reg} cells in the siLP. To determine whether such pT_{reg} cells can be selectively identified, we examined the expression of RAR (retinoic acid receptor)–related orphan receptor gamma t (RORγt), which is expressed by lymphocytes that interact with microbes (*16*). As previously reported (*17*), in SPF B6 mice, RORγt$^+$ T_{reg} cells were present in the siLP and cLP, mostly as Nrp-1^{lo} pT_{reg} cells (Fig. 3, A and B). In contrast, RORγt$^+$ T_{reg} cells were almost undetectable in GF and AF B6 mice (Fig. 3, A and B); RORγt$^+$ CD4$^+$ conventional T cells were similarly absent (fig. S10, A and B). The gut RORγt$^+$ T_{reg} cells rapidly appeared in GF mice after conventionalization (fig. S10, C and D). Moreover, treatment of SPF mice with a cocktail of antibiotics for 4

[1]Academy of Immunology and Microbiology, Institute for Basic Science, Pohang, Republic of Korea. [2]Department of Integrative Biosciences and Biotechnology, Pohang University of Science and Technology, Pohang, Republic of Korea. [3]Division of Developmental Immunology, La Jolla Institute for Allergy and Immunology, La Jolla, CA 92037, USA.
*Corresponding author. E-mail: csurh@ibs.re.kr

weeks from the time of weaning led to a depletion of RORγt$^+$ pT$_{reg}$ cells in the siLP and cLP, without affecting the generation of RORγt$^-$ pT$_{reg}$ cells (Fig. 3C). In addition, weaning SPF mice onto the Ag-free diet or an amino acid diet caused a severe reduction of Nrp-1^{lo} pT$_{reg}$ cells in the siLP, mostly due to a depletion of RORγt$^-$ pT$_{reg}$ cells (Fig. 3D and fig. S11). The bacterial load, but not the composition, in the feces of SPF mice that were weaned onto the Ag-free diet was relatively normal (fig. S12). Collectively, these findings add to recent reports (*18*, *19*) by showing that whereas RORγt$^+$ pT$_{reg}$ cells are induced by commensal microbiota, RORγt$^-$ pT$_{reg}$ cells are driven by dietary Ags.

We next examined the dendritic cell (DC) subsets in the intestines of AF mice. Unexpectedly, the siLP of AF mice contained a ~40% lower representation of the CD103$^+$ CD11b$^+$ subset that promotes pT$_{reg}$ cell development (*14*, *20*) and about three times the proportion of the CD103$^+$ CD11b$^-$ subset, relative to SPF and GF mice, resembling conventional splenic DCs (fig. S13, A to C) (*21*). However, such a skewed DC composition only partially explains the paucity of pT$_{reg}$ cells in the intestines of AF mice. This is because a normal DC subset composition was found in the mesenteric lymph nodes of AF mice, which are the induction sites of pT$_{reg}$ cell development; moreover, purified CD103$^+$ CD11b$^+$ DCs from the siLP of AF mice were able to efficiently stimulate T cells (fig. S14, A and B) and induce upregulation of Foxp3 in OT-II cells under in vitro conditions (fig. S14, C and D). Furthermore, weaning neonatal AF or GF mice, which also possess the skewed DC subsets (fig. S13D), onto a chow diet led to the normalization of DC subsets within 1 week (fig. S13, D and E) and efficient development of pT$_{reg}$ cells within 2 weeks in the siLP (Fig. 2A). Lastly, siLP pT$_{reg}$ cells from neonatal AF mice weaned onto a chow diet exhibited ~50% demethylation at the CNS2 regions of the *Foxp3* locus (fig. S15), indicative of stable Foxp3 expression, as previously reported (*7*, *22*).

Despite the deficiency in siLP pT$_{reg}$ cells, B6 SPF or GF neonatal mice do not develop food allergies when they are weaned onto a chow diet. This could be due to various anti-inflammatory proteins in milk (*23*), such as immunoglobulins, transforming growth factor (TGF)–β, osteopontin, and lactadherin, which could ameliorate

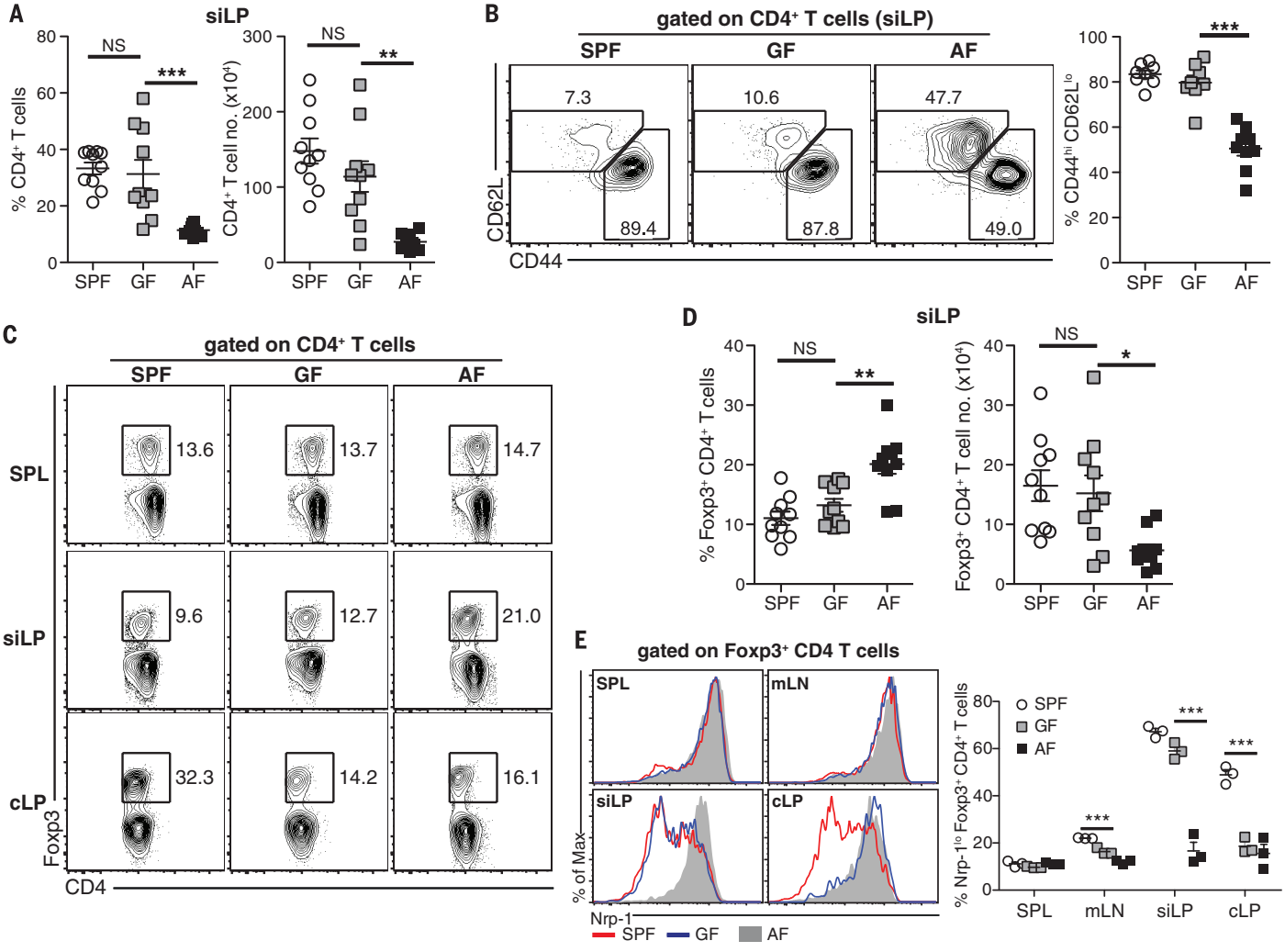

Fig. 1. Depletion of macromolecules from the diet precludes the development of pT$_{reg}$ cells in the small intestine. Shown are comparisons of T cell populations from the siLP and cLP harvested from aged-matched young adult (6- to 10-week-old) SPF, GF, and AF B6 mice. (**A**) CD4$^+$ T cells from the siLP, expressed as percentages of lymphocytes (left) and total numbers (right). (**B**) Representative fluorescence-activated cell sorting (FACS) plots of CD44 versus CD62L (numbers in the boxes indicate percentages of cells in the gate), with a graph of the percentages of CD44^{hi} CD62L^{lo} cells among the siLP CD4$^+$ T cells. (**C**) Representative FACS plots of CD4 versus Foxp3 on gated CD4$^+$ T cells from the spleen (SPL), siLP, and cLP. (**D**) Foxp3$^+$ CD4$^+$ T cells from the siLP are expressed as percentages of lymphocytes (left) and total numbers (right). (**E**) Representative histograms of Nrp-1 expression, with a graph of the percentages of Nrp-1^{lo} cells among gated Foxp3$^+$ CD4$^+$ T cells from the SPL, mesenteric lymph node (mLN), siLP, and cLP. At least four independent experiments had similar results. Graphs in (A), (B), and (D) show pooled data points from four independent experiments. *P* values were determined by one-way analysis of variance (ANOVA) with the Bonferroni post-test. Error bars show SEM. *$P < 0.05$; **$P < 0.01$; ***$P < 0.001$; NS, not significant.

the allergic response. We therefore examined the effect of feeding adult B6 AF mice a sterile chow diet; this failed to induce any gross sign of intestinal pathology. However, the initial local immune response to dietary Ags could be vigorous because of the absence of pT_{reg} cells and the increased numbers of siLP $CD103^+$ $CD11b^-$ DCs. Hence, we adoptively transferred ovalbumin (OVA)–specific naïve OT-II $CD4^+$ T cells into adult AF mice and then gave them OVA orally. Examination on day 7 revealed that OT-II cells in the siLP of AF mice expanded ~50 and 7 times as much as in control SPF and GF mice, respectively (Fig. 4A). Moreover, whereas the majority (~60%) of expanded OT-II cells upregulated Foxp3 in SPF and GF mice, only ~30% of OT-II cells up-regulated Foxp3 in AF mice (Fig. 4B).

The expanded OT-II cells in AF mice, some of which could be due to homeostatic proliferation, readily differentiated into $Tbet^+$ T helper 1 (T_h1) cells, leading to the generation of ~400 or ~14 times as many T_h1 cells as in SPF or GF mice, respectively; a similar trend, at smaller magnitudes, applied to interferon-γ^+ OT-II cells (Fig. 4C and fig. S16A). Moreover, the relative ratio of T_{reg} to T_h1 OT-II cell generation in AF mice was one-twentieth that in SPF mice (fig. S16B). Unlike the T_h1 response, T_h2 and T_h17 responses in AF hosts were comparable to that in control SPF hosts. Hence, whereas GF hosts had increased T_h2 responses to OVA, AF hosts possessed only background levels of OVA-specific and total serum immunoglobulin E (IgE), a minimal number of $GATA3^+$ OT-II cells, and a similarly moderate percentage of $ROR\gamma t^+$ OT-II cells as that observed in control SPF hosts (Fig. 4D and fig. S16, C to F). As expected, $Foxp3^+$ OT-II cells in AF hosts were mostly $Nrp\text{-}1^{lo}$ pT_{reg} cells and expressed higher levels of CTLA-4 and IL-10 than host T_{reg} cells, which were mostly tT_{reg} cells (fig. S17, A to C). Unexpectedly, the majority of $Foxp3^+$ OT-II cells were $ROR\gamma t^+$ (fig. S16, E and F), indicating that dietary proteins can induce the development of $ROR\gamma t^+$ pT_{reg} cells from a fraction of the T cell repertoire in the absence of the commensal microbiota. Nonetheless, the major characteristics of the OT-II response observed in the siLP of AF

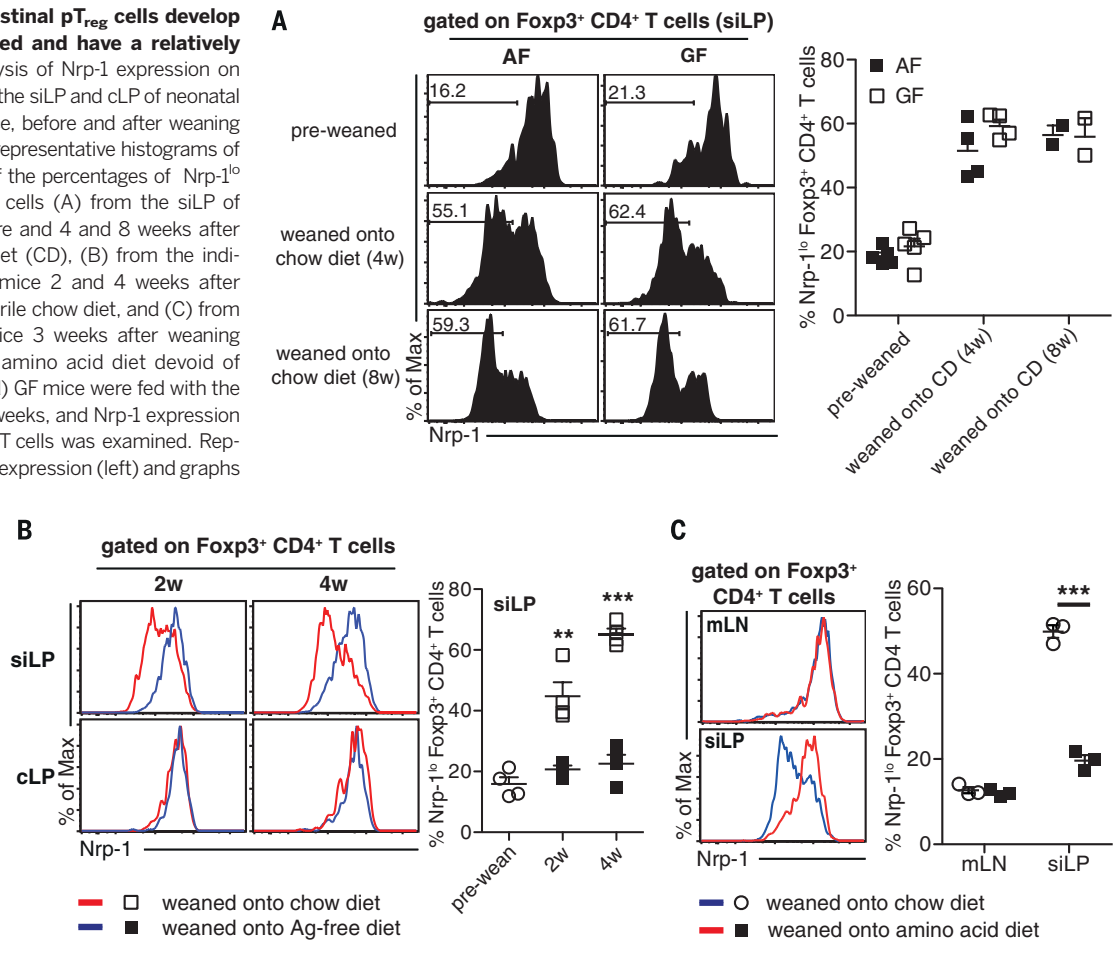

Fig. 2. The bulk of small intestinal pT_{reg} cells develop when solid food is introduced and have a relatively short life span. (**A** to **C**) Analysis of Nrp-1 expression on gated $Foxp3^+$ $CD4^+$ T cells from the siLP and cLP of neonatal (3-week-old) GF and AF B6 mice, before and after weaning onto a specific diet. Shown are representative histograms of Nrp-1 expression, with graphs of the percentages of $Nrp\text{-}1^{lo}$ cells on gated $Foxp3^+$ $CD4^+$ T cells (A) from the siLP of neonatal GF and AF mice before and 4 and 8 weeks after weaning onto a sterile chow diet (CD), (B) from the indicated tissues of neonatal GF mice 2 and 4 weeks after weaning onto the Ag-free or sterile chow diet, and (C) from the indicated tissues of GF mice 3 weeks after weaning onto a sterile chow diet or an amino acid diet devoid of proteins. (**D**) Adult (8-week-old) GF mice were fed with the Ag-free diet (AFD) for 2 and 4 weeks, and Nrp-1 expression on siLP and cLP $Foxp3^+$ $CD4^+$ T cells was examined. Representative histograms of Nrp-1 expression (left) and graphs of percentages and numbers (right) of $Nrp\text{-}1^{lo}$ $Foxp3^+$ $CD4^+$ T cells are shown. Graphs in (A), (B), and (D) show combined data points from two independent experiments. The graph in (C) is representative of two independent experiments. *P* values were determined by two-tailed unpaired Student's *t* tests [(B) and (C)] and one-way ANOVA with the Bonferroni post-test (D). Error bars show SEM. $*P < 0.05$; $**P < 0.01$; $***P < 0.001$.

hosts were also evident in the mesenteric lymph nodes, but not in the spleen, indicating that the pronounced OVA-driven OT-II cell response in AF mice is restricted to the gut-associated lymphoid tissues. The massive OT-II response in AF hosts also was not due to more efficient Ag presentation of OVA related to a lack of competition from other proteins or low vitamin A levels, because similar T cell expansion occurred in a group of AF mice that were fed with a sterilized chow diet just before introducing OVA or injected with retinoic acid during OVA feeding (fig. S18). Overall, these findings indicate that siLP pT_{reg} but not tT_{reg} cells are essential to suppressing a default strong immune response to newly introduced dietary Ags.

Lastly, based on the OT-II response observed above, we tested whether food allergies can be induced in an experimental model. Hence, neonatal SPF BALB/c mice were weaned onto an amino acid diet (because B6 mice are generally resistant to food allergies) and immunized with OVA. Two weeks later, repeated gavage with OVA led to a higher incidence and severity of diarrhea, with a trend toward higher OVA-specific serum IgE, in the amino acid diet–fed mice than in control mice (Fig. 4E and fig. S19). Hence, the lack of pT_{reg} cells led to an increased susceptibility to OVA-induced intestinal allergy.

Our work demonstrates that under normal physiological conditions, macromolecules from the diet induce the bulk of pT_{reg} cell development in the siLP, but not in the cLP. Most siLP pT_{reg} cells develop after weaning onto solid food, presumably reflecting the limited antigenic complexity of milk, an immature state of the immune system in neonatal mice, and/or the presence of components exclusively found in solid food that boost pT_{reg} cell development. The expansion of

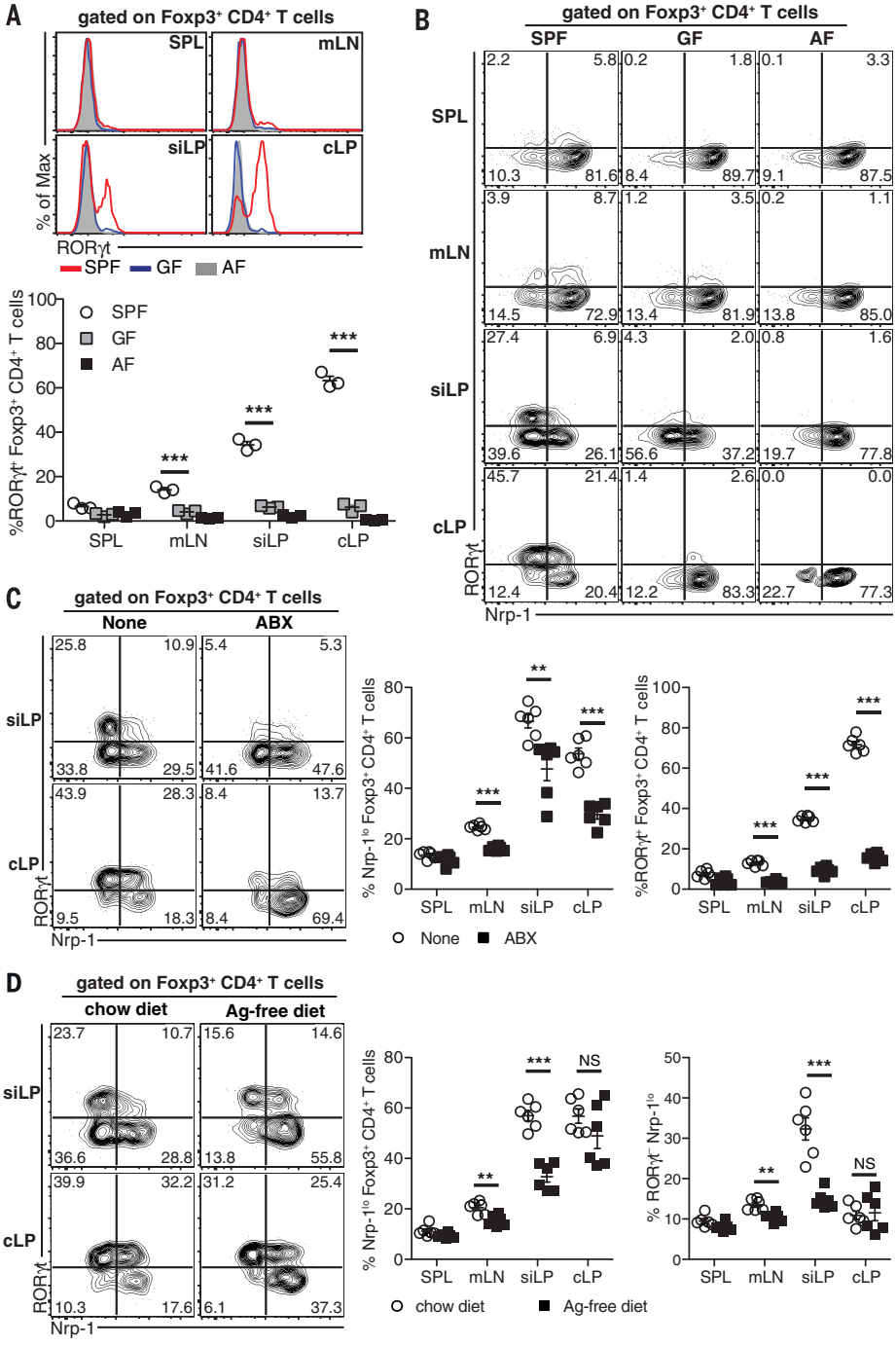

Fig. 3. Under normal conditions, a subset of small intestinal pT_{reg} cells is induced to develop by the commensal microbiota and expresses RORγt. Shown are analyses of RORγt expression on gated Foxp3$^+$ CD4$^+$ T cells from the siLP and cLP of young adult SPF, GF, and AF B6 mice [(A) and (B)] or on SPF mice after treatment with antibiotics or after weaning onto an Ag-free diet [(C) and (D)]. (**A**) Representative histograms of RORγt expression, with a graph of the percentages of RORγt$^+$ cells among gated Foxp3$^+$ CD4$^+$ T cells from the SPL, mLN, siLP, and cLP of SFP, GF, and AF mice. (**B**) Representative FACS plot of Nrp-1 versus RORγt on gated Foxp3$^+$ CD4$^+$ T cells from the indicated tissues and mice. (**C** and **D**) Representative FACS plots of Nrp-1 versus RORγt, with graphs of the percentages of Nrp-1^{lo} (left) and RORγt$^+$ cells (right) among Foxp3$^+$ CD4$^+$ T cells in the siLP and cLP of recently weaned SFP mice; the mice were given water with or without broad-spectrum antibiotics (ABX) (C) or a chow diet or Ag-free diet (D) for 4 weeks. The graph in (A) is representative of at least two independent experiments, and graphs in (C) and (D) show combined data points from two independent experiments. *P* values were determined by one-way ANOVA with the Bonferroni post-test in (A) and by two-tailed unpaired Student's *t* tests or *t* tests with Welch's correction in case of unequal variance in (C) and (D). Error bars show SEM. $*P < 0.05$; $**P < 0.01$; $***P < 0.001$.

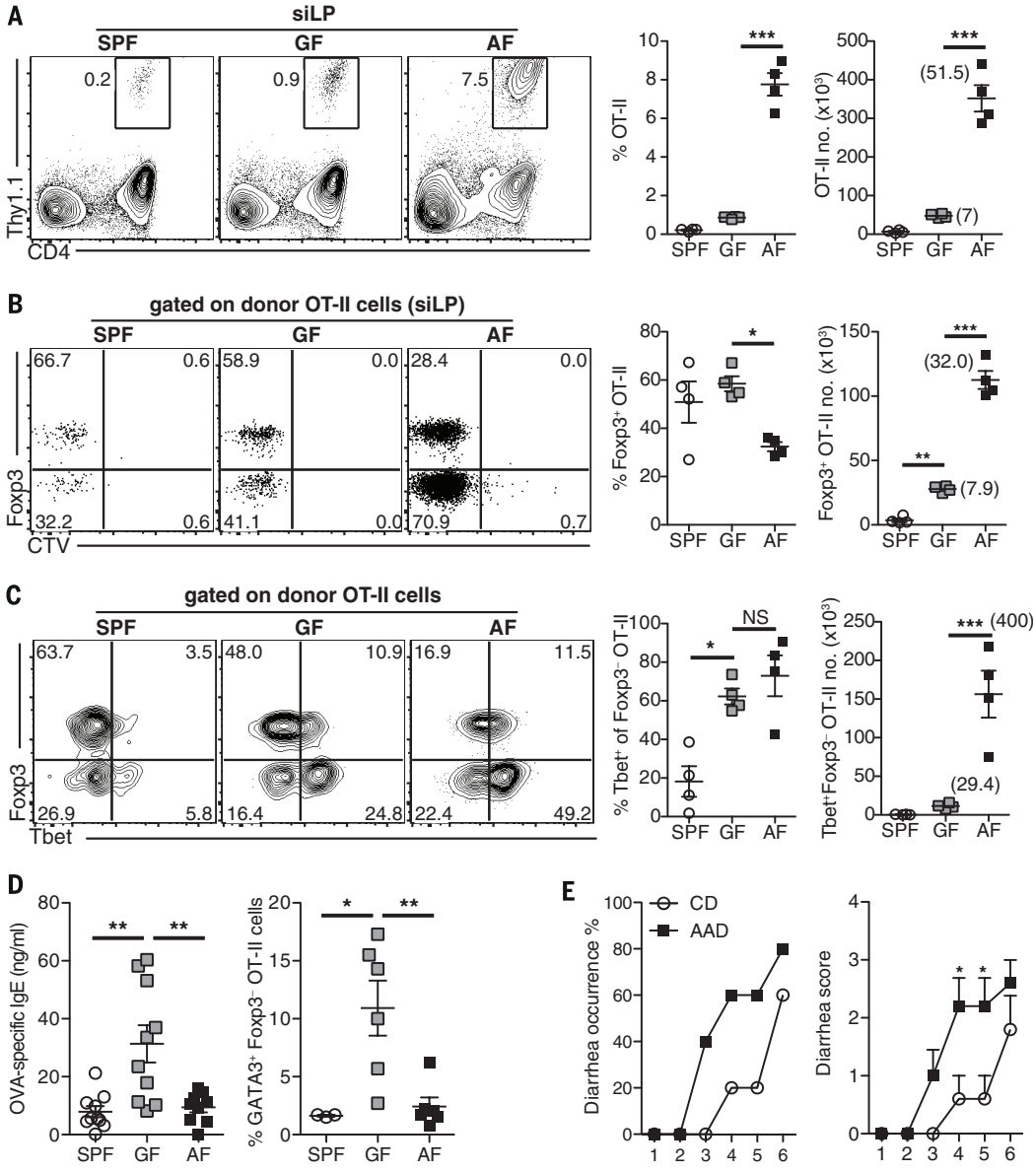

Fig. 4. Conditions in which pT_{reg} cells are depleted allow strong immune responses to dietary antigens and an increased susceptibility to intestinal allergy. In (A) to (D), adult SPF, GF, and AF B6 mice (N = 4 per group) were adoptively transferred with Cell Trace Violet–labeled naïve Thy1$^+$ OT-II cells and fed with OVA for 7 days; donor OT-II cells from the siLP were then analyzed along with serum IgE specific to OVA. (**A**) OT-II cells in representative FACS plots of all lymphocytes, with graphs of percentages (left) and total numbers (right) of OT-II cells. (**B**) Foxp3 up-regulation in OT-II cells in representative FACS plots of gated OT-II cells, with graphs of percentages (left) and total numbers (right) of Foxp3$^+$ OT-II cells. (**C**) Tbet up-regulation in OT-II cells in representative FACS plots of gated OT-II cells, with graphs of percentages (left) and total numbers (right) of Tbet$^+$ Foxp3$^-$ OT-II cells. (**D**) Graphs of serum OVA-specific IgE (left) and percentages of GATA3$^+$ Foxp3$^-$ OT-II cells (right). (**E**) Neonatal SPF BALB/c mice were weaned onto a normal chow diet or an amino acid diet (AAD), immunized with OVA plus alum, rested for 2 weeks, gavaged with OVA on an every-other-day basis, and observed for diarrhea. Graphs of percentages of mice with diarrhea (left) and diarrhea scores (right) (N = 5 per group). In the graphs in (A) to (C), the numbers in parentheses denote the fold of cell expansion above that found in SPF hosts. Graphs in (A), (B), and (E) are representative of at least two independent experiments, and graphs in (D) show pooled data points from at least two independent experiments. P values were determined by one-way [(A) to (D)] or two-way (E) ANOVA with the Bonferroni post-test. Error bars show SEM. *P < 0.05; **P < 0.01; ***P < 0.001.

siLP pT_{reg} cells after weaning appears to be essential to suppressing a default strong immune response to dietary Ags, supporting the view that pT_{reg} cells are important for controlling mucosal inflammatory and allergic responses (*6*, *10*, *24*). The data could also explain why children suffer from a higher incidence of food allergies than adults do and why childhood allergies spontaneously dissipate with time (*25*). Nevertheless, despite their lack of siLP pT_{reg} cells, most neonates do not exhibit food allergies. Such tolerance might reflect multiple mechanisms, including efficient pT_{reg} cell induction by the high levels of TGF-β in milk (*23*), compensatory suppression by tT_{reg} cells, and/or rapid generation of pT_{reg} cells induced by commensal microbial Ags. For the last of these, it is known that germ-free mice spontaneously produce large amounts of IgE and that this can be prevented by colonization with a complex commensal microbiota (*26*, *27*). Hence, the presence of both diet- and microbe-induced populations of pT_{reg} cells may be required for complete tolerance to food Ags.

REFERENCES AND NOTES

1. H. L. Weiner, A. P. da Cunha, F. Quintana, H. Wu, *Immunol. Rev.* **241**, 241–259 (2011).
2. O. Pabst, A. M. Mowat, *Mucosal Immunol.* **5**, 232–239 (2012).
3. A. M. Bilate, J. J. Lafaille, *Annu. Rev. Immunol.* **30**, 733–758 (2012).
4. K. Kretschmer *et al.*, *Nat. Immunol.* **6**, 1219–1227 (2005).
5. D. Mucida *et al.*, *J. Clin. Invest.* **115**, 1923–1933 (2005).
6. D. Haribhai *et al.*, *Immunity* **35**, 109–122 (2011).
7. J. M. Weiss *et al.*, *J. Exp. Med.* **209**, 1723–1742 (2012).
8. Y. Furusawa *et al.*, *Nature* **504**, 446–450 (2013).
9. N. Arpaia *et al.*, *Nature* **504**, 451–455 (2013).
10. U. Hadis *et al.*, *Immunity* **34**, 237–246 (2011).
11. J. R. Pleasants, M. H. Johnson, B. S. Wostmann, *J. Nutr.* **116**, 1949–1964 (1986).
12. P. Pereira *et al.*, *Eur. J. Immunol.* **16**, 685–688 (1986).
13. B. S. Wostmann, J. R. Pleasants, *Proc. Soc. Exp. Biol. Med.* **198**, 539–546 (1991).
14. J. L. Coombes *et al.*, *J. Exp. Med.* **204**, 1757–1764 (2007).
15. D. Mucida *et al.*, *Science* **317**, 256–260 (2007).
16. G. Eberl, *Immunol. Rev.* **245**, 177–188 (2012).
17. M. Lochner *et al.*, *J. Exp. Med.* **205**, 1381–1393 (2008).
18. C. Ohnmacht *et al.*, *Science* **349**, 989–993 (2015).
19. E. Sefik *et al.*, *Science* **349**, 993–997 (2015).
20. C. M. Sun *et al.*, *J. Exp. Med.* **204**, 1775–1785 (2007).
21. K. Fujimoto *et al.*, *J. Immunol.* **186**, 6287–6295 (2011).

22. J. K. Polansky *et al.*, *Eur. J. Immunol.* **38**, 1654–1663 (2008).
23. D. E. Chatterton, D. N. Nguyen, S. B. Bering, P. T. Sangild, *Int. J. Biochem. Cell Biol.* **45**, 1730–1747 (2013).
24. S. Z. Josefowicz *et al.*, *Nature* **482**, 395–399 (2012).
25. G. Longo, I. Berti, A. W. Burks, B. Krauss, E. Barbi, *Lancet* **382**, 1656–1664 (2013).
26. J. Cahenzli, Y. Köller, M. Wyss, M. B. Geuking, K. D. McCoy, *Cell Host Microbe* **14**, 559–570 (2013).
27. K. D. McCoy *et al.*, *Immunity* **24**, 329–339 (2006).

ACKNOWLEDGMENTS

We thank A. Macpherson, K. McCoy, and D. Artis for generously providing various strains of germ-free mice to start our colony; T. K. Kim, J. W. Seo, M. O. Lee, H. J. Woo, H. J. Jung, H.J. Ko, J. Kirundi, S. Sakaguchi, and N. Ohkura for technical support; and J. Sprent, S. H. Im, M. H. Jang, D. Rudra, and J. H. Cho for discussions. The data from this study are tabulated in the main paper and in the supplementary materials. This work was supported by project IBS-R005-D1 of the Institute for Basic Science, Korean Ministry of Science, Information/Communication Technology and Future Planning.

SUPPLEMENTARY MATERIALS

www.sciencemag.org/content/351/6275/858/suppl/DC1
Materials and Methods
Figs. S1 to S19
Table S1
References (*28*–*32*)

14 May 2015; accepted 5 January 2016
Published online 28 January 2016
10.1126/science.aac5560

ION CHANNELS

Sequential ionic and conformational signaling by calcium channels drives neuronal gene expression

Boxing Li,[1]* Michael R. Tadross,[2,3]*† Richard W. Tsien[1,2]

Voltage-gated $Ca_V1.2$ channels (L-type calcium channel α1C subunits) are critical mediators of transcription-dependent neural plasticity. Whether these channels signal via the influx of calcium ion (Ca^{2+}), voltage-dependent conformational change (VΔC), or a combination of the two has thus far been equivocal. We fused $Ca_V1.2$ to a ligand-gated Ca^{2+}-permeable channel, enabling independent control of localized Ca^{2+} and VΔC signals. This revealed an unexpected dual requirement: Ca^{2+} must first mobilize actin-bound Ca^{2+}/calmodulin-dependent protein kinase II, freeing it for subsequent VΔC-mediated accumulation. Neither signal alone sufficed to activate transcription. Signal order was crucial: Efficiency peaked when Ca^{2+} preceded VΔC by 10 to 20 seconds. $Ca_V1.2$ VΔC synergistically augmented signaling by *N*-methyl-D-aspartate receptors. Furthermore, VΔC mistuning correlated with autistic symptoms in Timothy syndrome. Thus, nonionic VΔC signaling is vital to the function of $Ca_V1.2$ in synaptic and neuropsychiatric processes.

Voltage-gated $Ca_V1.2$ channels (L-type calcium channel α1C subunits) play an important role in transcription-dependent forms of synaptic and homeostatic plasticity (*1*–*6*), and $Ca_V1.2$ alterations have been linked to severe neuropathologies (*7*, *8*). The influx of Ca^{2+} is required in $Ca_V1.2$-mediated transcription (*4*), but it remains unclear whether voltage-dependent conformational change (VΔC) provides a necessary additional signal. There is precedence for VΔC signaling: $Ca_V1.1$ uses only VΔC to initiate skeletal-muscle contraction (*9*, *10*). However, a signaling role for VΔC has been difficult to establish in excitation-transcription coupling, because eliminating voltage-dependent opening of the channel also prevents Ca^{2+} influx through the Ca_V [but see (*11*)].

We fused $Ca_V1.2$ to an adenosine triphosphate (ATP)–gated, Ca^{2+}-permeable, tandem-trimeric P2X2 channel (ttP2X) (Fig. 1A). The ttP2X was used to provide Ca^{2+} influx independently of whether $Ca_V1.2$ was open or closed; the tethering between the channels (Fig. 1A) localized ttP2X influx to the $Ca_V1.2$ nanodomain (*12*, *13*).

We confirmed the integrity of the chimeric protein and the functionality of its components (fig. S1). In human embryonic kidney (HEK) 293 cells, the Ca^{2+} current appeared only at depolarized potentials in the absence of ATP (Fig. 1B, black u-shaped trace), as expected for a voltage-gated $Ca_V1.2$. On addition of ATP, the ttP2X portion of the chimera also supported Ca^{2+} influx, evident as an additional inward current at negative potentials (Fig. 1B, gray trace). Cd^{2+}, which blocks the $Ca_V1.2$ pore (*14*) but not the opening of ttP2X, did not prevent the ttP2X-mediated entry of Ca^{2+} (Fig. 1B, blue trace). We further validated the function of the chimeric components in cultured neurons, rendering the $Ca_V1.2$ portion dihydropyridine-insensitive (DHPi) to enable its distinction from endogenous channels (*6*) and confirming that ATP had no effect on untransfected neurons (fig. S1). Whereas ttP2X on its own distributed uniformly over the somatodendritic surface, ttP2X fused to $Ca_V1.2$ formed puncta and signaled more potently (fig. S1), consistent with localization to signaling hotspots.

These control experiments framed critical tests of the roles of Ca^{2+} and VΔC in signaling to nuclear CREB (cyclic adenosine monophosphate response–element binding protein), a transcription factor that is critical in many forms of learning and memory (Fig. 1, D and E) (*1*, *2*, *15*). Providing Ca^{2+} and VΔC in combination via the depolarization of neurons (3 min of exposure to 40 mM K^+ ($40K^+$)] (Fig. 1C, black traces) increased the phosphorylation of nuclear CREB (pCREB) at Ser^{133} threefold (Fig. 1D, second row) (*3*–*5*). The pCREB response was abolished by Cd^{2+} (Fig. 1D, third row), which prevents $Ca_V1.2$ from conducting Ca^{2+} without affecting depolarization (Fig. 1C, gray traces) or voltage-dependent gating (*14*); this confirms the known requirement for Ca^{2+} influx in signaling to pCREB (*4*, *6*, *13*). Next, we rerouted Ca^{2+} through the neighboring ttP2X by blocking the $Ca_V1.2$ pore with Cd^{2+} and opening the ttP2X portion of the chimera with ATP. This generated depolarizations and increases in bulk Ca^{2+} that were nearly identical to those achieved with $40K^+$ (Fig. 1C, compare blue with black traces, and fig. S2, A and B) and increased pCREB to the same degree as $40K^+$ (compare Fig. 1E, top row, with Fig. 1D, second row), confirming the utility of the chimeric channel approach.

We thus could use the chimera to determine whether localized Ca^{2+} influx can drive CREB activation in the absence of VΔC. In a first test, we provided the localized influx of Ca^{2+} by means of ATP activation of the chimeric ttP2X, but we attenuated VΔC signals through hyperpolarization, which was achieved by coexpressing and activating an ivermectin-gated chloride channel (GlyIVR) (*16*). This manipulation prevented neuronal depolarization (fig. S2C) and thus increased Ca^{2+} flux through the chimeric ttP2X (Fig. 1B, blue). Nonetheless, this manipulation inhibited signaling to CREB (Fig. 1E, second row). The attenuation of CREB signaling required a combination of GlyIVR expression and ivermectin (fig. S2D) and could not be attributed to increased Ca^{2+} influx (fig. S2E).

In a second test, we inhibited $Ca_V1.2$ conformational opening with nimodipine. This Ca_V1-selective agent (*17*, *18*) blocked ATP-mediated CREB signaling (Fig. 1E, third row) without affecting depolarization or Ca^{2+} influx (Fig. 1C, compare orange with blue). Nimodipine did not block the pCREB response when the chimeric $Ca_V1.2$ was rendered nimodipine-insensitive (Fig. 1E, bottom row), excluding potential off-target effects of the drug. Similar results were obtained with CREB-dependent expression of the immediate early gene *c-fos* (fig. S3). Thus, $Ca_V1.2$ signaling to pCREB and gene expression requires two distinct messages: The Ca^{2+} signal works in conjunction with an equally indispensable VΔC signal arising from $Ca_V1.2$.

[1]Department of Neuroscience and Physiology and New York University Neuroscience Institute, New York, NY 10016, USA. [2]Department of Molecular and Cellular Physiology, Beckman Center, School of Medicine, Stanford University, Stanford, CA 94305, USA. [3]Janelia Research Campus, Howard Hughes Medical Institute, Ashburn, VA 20147, USA.
*These authors contributed equally to this work. †Corresponding author. E-mail: tadrossm@janelia.hhmi.org

Dietary antigens limit mucosal immunity by inducing regulatory T cells in the small intestine

Kwang Soon Kim *et al.*

Science **351**, 858 (2016);
DOI: 10.1126/science.aac5560